



CHICAGO JOURNALS



The University of Chicago

The Effects of the Avoidance of Infectious Hosts on Infection Risk in an Insect-Pathogen Interaction.

Author(s): Libby Eakin, Mei Wang, and Greg Dwyer

Source: *The American Naturalist*, Vol. 185, No. 1 (January 2015), pp. 100-112

Published by: [The University of Chicago Press](http://www.press.uchicago.edu) for [The American Society of Naturalists](http://www.asn-online.org)

Stable URL: <http://www.jstor.org/stable/10.1086/678989>

Accessed: 06/01/2015 10:22

Your use of the JSTOR archive indicates your acceptance of the Terms & Conditions of Use, available at <http://www.jstor.org/page/info/about/policies/terms.jsp>

JSTOR is a not-for-profit service that helps scholars, researchers, and students discover, use, and build upon a wide range of content in a trusted digital archive. We use information technology and tools to increase productivity and facilitate new forms of scholarship. For more information about JSTOR, please contact support@jstor.org.



The University of Chicago Press, The American Society of Naturalists, The University of Chicago are collaborating with JSTOR to digitize, preserve and extend access to *The American Naturalist*.

<http://www.jstor.org>

The Effects of the Avoidance of Infectious Hosts on Infection Risk in an Insect-Pathogen Interaction

Libby Eakin,¹ Mei Wang,² and Greg Dwyer^{1,*}

1. Department of Ecology and Evolution, University of Chicago, Chicago, Illinois 60637; 2. Department of Statistics, University of Chicago, Chicago, Illinois 60637

Submitted September 23, 2013; Accepted June 18, 2014; Electronically published November 19, 2014

Online enhancement: appendix. Dryad data: <http://dx.doi.org/10.5061/dryad.q6h4n>.

ABSTRACT: In many animal host-pathogen interactions, uninfected hosts either avoid or are attracted to infected conspecifics, but understanding how such behaviors affect infection risk is difficult. In experiments, behaviors are often eliminated entirely, which allows demonstration that a behavior affects risk but makes it impossible to quantify effects of individual behaviors. In models, host behaviors have been studied using ordinary differential equations, which can be easily analyzed but cannot be used to relate individual behaviors to risk. For many insect baculoviruses, however, quantifying effects of behavior on risk is straightforward because transmission occurs when host larvae accidentally consume virus-contaminated foliage. Moreover, increases in computing power have made it possible to fit complex models to data. We therefore used experiments to quantify the behavior of gypsy moth larvae feeding on oak leaves contaminated with virus-infected cadavers, and we tested for effects of cadaver-avoidance behavior by fitting stochastic simulation models to our data. The models that best explain the data include cadaver avoidance, and comparison of models that do and do not include cadaver avoidance shows that this behavior substantially reduces infection risk. Our work demonstrates that host behaviors that affect exposure risk play a key role in baculovirus transmission and adds to the growing consensus that host behavior can strongly alter pathogen transmission rates.

Keywords: *Lymantria dispar*, host-pathogen interaction, host behavior, nucleopolyhedrovirus, disease ecology, behavior and disease.

Introduction

In many animal host-pathogen interactions, uninfected hosts either avoid or are attracted to infected conspecifics (Hawley et al. 2011). Attraction and avoidance behaviors likely play a key role in the spread of disease within populations, and so understanding the consequences of these behaviors for infection risk is an important area of current research (Antolin 2008). The complexity of such behaviors,

however, means that both empirical and theoretical research approaches face significant obstacles.

First, experiments have been used to demonstrate that host avoidance behaviors can alter infection risk but typically only by eliminating the behavior of interest. For example, Kiesecker et al. (1999) showed that uninfected bullfrog (*Rana catesbeiana*) tadpoles avoid conspecifics infected with the fungal pathogen *Candida humicola*. To demonstrate that this behavior reduces risk, the authors confined uninfected hosts at a range of distances from an infected conspecific to show that risk falls with distance from an infected host. Similarly, Behringer et al. (2006) showed that Caribbean spiny lobsters (*Panulirus argus*) avoid conspecifics infected with the species-specific *Panulirus argus* virus. To again demonstrate that the avoidance behavior reduces infection risk, the authors confined infected and uninfected hosts together in the laboratory to show that proximity produces infection rates that are substantially higher than those observed in the field. These experiments strongly suggest that avoidance reduces infection risk, but they do not allow for an understanding of how infection rates are determined by individual behaviors, such as changes in movement rate or turning angle in response to the presence of an infected conspecific.

Second, mathematical models have provided invaluable guidance in disease ecology (Keeling and Rohani 2007), but most disease models consist of ordinary differential equations that track host densities or numbers over time (Anderson and May 1992), whereas mechanistic models of behavior must additionally track densities or numbers over space and how densities or numbers affect movement behavior. These latter complications require either partial differential equations (Kareiva and Odell 1987) or complex computer algorithms (Longini et al. 2005), and so standard models are of limited usefulness for understanding the consequences of individual host behaviors for infection risk. Standard models have nevertheless played an important role in managing diseases for which host behaviors

* Corresponding author; e-mail: gdwyer@uchicago.edu.

are relatively simple (Keeling and Rohani 2007), suggesting that the lack of models that allow for complex behaviors may hinder disease management.

For example, Hosseini et al. (2004) used ordinary differential equation models to study the dynamics of mycoplasmal conjunctivitis (*Mycoplasma gallisepticum*) in house finches (*Carpodacus mexicanus*) in North America. The models that best describe infection rate data allow for periodic increases in transmission as a phenomenological description of the seasonal flocking behavior that occurs independently of infection status. Later experiments showed that uninfected hosts prefer to associate with infected conspecifics, presumably because sick individuals are less aggressive (Bouwman and Hawley 2010), but such attraction behavior is not well described by the seasonally fluctuating transmission in the Hosseini et al. model. Hawley et al. (2011) therefore constructed an ordinary differential equation model that allows for attraction behavior in terms of covariation between mean susceptibility and mean contact rates, but the resulting model does not express infection risk in terms of individual behaviors.

Here we combine the strengths of the experimental and modeling approaches to understand the effects of host avoidance behavior on the risk of baculovirus infection in the gypsy moth (*Lymantria dispar*). Insect baculoviruses are convenient for studying the effects of host behavior on pathogen transmission because transmission in many insects occurs when host larvae accidentally consume foliage contaminated with the infectious cadavers of conspecifics (Cory and Myers 2003). It is therefore possible to directly observe transmission events, which in turn makes it possible to quantify host behaviors that alter infection risk (Dwyer et al. 2005). Moreover, previous choice tests have shown that gypsy moth larvae prefer uncontaminated foliage to cadaver-contaminated foliage, suggesting that avoidance of infectious cadavers is an important means by which gypsy moth larvae reduce their infection risk (Capinera et al. 1976; Parker et al. 2010). Choice tests, however, leave an important question unanswered: does cadaver-avoidance behavior actually reduce a gypsy moth larva's risk of infection?

To answer this question, we constructed a model that included avoidance behavior, and we tested whether it provided a better explanation for data from laboratory feeding experiments than a model that did not include avoidance behavior. As in previous experiments (Kiesecker et al. 1999; Behringer et al. 2006), infected and uninfected hosts in our experiments were confined in an arena of limited area, but the spatial scale over which gypsy moth larvae avoid cadavers is small enough that the arenas nevertheless appeared to allow for natural feeding, and models based on the experiments predict infection rates in the field with reasonable accuracy. As in previous modeling

studies (Hosseini et al. 2004), we quantified the consequences of avoidance behavior on infection risk by comparing the predictions of models with and without the behavior, but we explicitly allowed for spatial structure and mechanistic feeding behavior, and so our models consist of stochastic simulation algorithms. We then used the corrected Akaike information criterion (AICc; Burnham and Anderson 2002) to show that the model that best explains the data includes cadaver avoidance. We thus follow Civitello et al. (2013), who similarly used model selection to show that feeding behavior affects the risk that *Daphnia dentifera* consume and become infected with a fungal pathogen, with the difference that Civitello et al.'s models include only feeding rates, whereas our models additionally allow individual hosts to decide where to feed.

To choose the best model, we first photographed the feeding patterns produced by individual larvae on virus-contaminated leaves and then recorded whether each larva subsequently became infected. We next constructed models that predict both the pattern of feeding and the probability of infection for each larva and then used maximum likelihood to fit the models to our data. Next, we used AICc analysis to show that the best model assumes that larvae can sometimes detect and avoid infectious cadavers. As evidence that our experiments did indeed allow for roughly realistic behavior, we show that the best model can successfully predict the outcome of previous field experiments (Elder et al. 2008). Finally, by comparing the predictions of models that do and do not include cadaver avoidance, we show that avoidance behavior substantially reduces a gypsy moth larva's infection risk. Our work provides important support for the hypothesis that pathogen transmission rates are often altered by host behaviors (Antolin 2008; Hawley et al. 2011), and our results have implications for the use of baculoviruses in insect pest control (Moreau and Lucarotti 2007).

Our models of overall infection risk include submodels that predict, first, the probability of infection given exposure and, second, the probability of exposure. Because the submodels were fit separately to different features of the experimental data, we first describe the laboratory experiments that produced the data, then how we fit each submodel to the data, and finally how we combined the two submodels and tested the resulting model predictions using data from field experiments. Each of the modeling sections, therefore, has its own methods and results sections.

Natural History and Experimental Methods

In North America, the gypsy moth is an invasive, outbreaking pest of hardwood forests (McManus and McIntyre 1981; Elkinton and Liebhold 1990). Gypsy moth outbreak cycles are driven partly by epizootics of the nu-

cleopolyhedrovirus *LdMNPV* (Woods and Elkinton 1987; Dwyer et al. 2004), a species-specific baculovirus that is used as an environmentally benign microbial insecticide (Webb et al. 1990, 2005). Previous choice tests showed that larvae prefer to feed on uncontaminated foliage rather than on cadaver-contaminated foliage (Capinera et al. 1976) and that this behavior is heritable (Parker et al. 2011). In choice tests, however, leaf material is presented to larvae in the form of small pieces of leaf that are either entirely contaminated or entirely uncontaminated, whereas in nature, larvae feed on entire leaves, and typically only a small fraction of a leaf is contaminated with cadavers. As in experiments with other host-pathogen systems (Kiesecker et al. 1999; Behringer et al. 2006), choice tests thus do not allow for an understanding of how individual behaviors determine infection risk.

In our experiments, we therefore instead allowed larvae to feed for 24 h on fully developed leaves in plastic clamshell boxes (note that we carried out two replicate experiments; see appendix, available online, for experimental details). This allowed us to quantify how close to a cadaver a larva must feed before it can detect and avoid the cadaver and how close it must feed to a cadaver in order to become infected. The boxes are smaller than the area within which a gypsy moth larva may move over 24 h in the field, but larvae nevertheless appeared to feed normally. Moreover, as we will show, our model provides a priori predictions of infection rates that are close to data from field experiments. Our data thus consist of leaf photographs before and after feeding and the postfeeding infection status of each larva.

We next used the image analysis program ImageJ to create a composite of each pre- and postfeeding photograph (<http://rsbweb.nih.gov/ij/>; appendix). Each composite image shows both the intact leaf and the area eaten by the larva (fig. A2; figures A1–A8 are available in the online appendix). These images allowed us to first confirm that the total area eaten and the number of feeding bouts did not differ between larvae that fed on uncontaminated control leaves and larvae that fed on cadaver-contaminated leaves (appendix). Feeding is therefore unaffected by overall contamination on a leaf, implying that infection risk is determined by feeding behavior at a spatial scale smaller than that of an entire leaf.

Modeling the Probability of Infection Given Exposure

Our overall goal was to infer how infection risk is affected by larval feeding behavior, which effectively determines exposure risk. To quantify the effects of exposure on infection risk, however, it was also necessary to quantify the probability of infection given exposure. Therefore, we first

used our data to choose between competing mechanistic models of the probability of infection given exposure.

Data on the probability of infection given exposure are often analyzed using generalized linear models (GLMs; Bolker et al. 2009; Bouwman and Hawley 2010; Parker et al. 2011). GLMs were insufficient for our purposes, however, because to understand feeding behavior, we had to take into account the spatial structure inherent in the infection process (D'Amico et al. 2005), which cannot be easily included in a GLM. For example, depending on the distribution of virus on a leaf, a larva that consumes a small amount of leaf tissue close to a cadaver could have a lower risk of infection than a larva that consumes a larger amount of leaf tissue farther away from the cadaver. Explicitly allowing for this effect using a GLM is difficult, but it is straightforward using a mechanistic model. Two of our simpler models are nevertheless almost identical to GLMs, but reassuringly in both cases, the GLM and the mechanistic model have very similar AICc scores (appendix).

Models

To fit models to our data, we first converted the 235 leaf images from our experiments into numerical grids. Because the photographs consist of pixels, it was straightforward to discretize the area of a leaf into cells of uniform area that preserved the relative size and shape of the leaf, the cadavers on the leaf, and the feeding bouts on the leaf. For ease of manipulation, the grids were also shrunk by half, again in a manner that preserved shapes and sizes (fig. A1).

We then assumed that a single larval bite is equal to the area of a grid cell (0.1 mm^2), an assumption that is justified by the ability of the resulting model to produce realistic feeding bouts and estimates of infection risk. We then created five models of the probability of infection given exposure, and we used the data to choose the best model. Recommended practice in model selection is to consider a reasonably small set of biologically plausible models to reduce the risk of selecting an incorrect model by chance (Burnham and Anderson 2002). We therefore considered a small number of models that were based on many hours of observations of gypsy moth larval feeding.

First, to allow for the possibility that feeding history had no effect on infection risk, we constructed a null model with no effects of either feeding behavior or spatial structure. In this model, the probability of infection P_j for larva j is the overall fraction infected in the experiments, so that $P_j = 51/235 = .217$ for all j , where 51 is the total number infected and 235 is the total number of insects.

We next constructed a model that includes the minimum distance that a larva fed from a cadaver. In this

Table 1: Corrected Akaike information criterion (AICc) scores, maximum likelihood estimates, and bootstrapped 95% confidence intervals (CIs) for our probability of infection models, in order of increasing AICc score

Model	AICc	ΔAICc	AICc weights	Parameters	95% CI
Closest distance to cadaver (nonlinear) + area eaten $P_j = 1 - \prod_{s=1}^{S_j} (1/1 + e^{-\alpha x_s^{\omega-\beta}})$	227.77	.0	.806	$\alpha = 2.98,$ $\beta = 4.37,$ $\omega = .195$	(.65, 5.42), (3.01, 6.95), (.022, .45)
Minimum distance eaten to a cadaver (nonlinear) $P_j = 1 - (1/1 + e^{-\alpha x_j^{\omega-\beta}})$	230.64	2.87	.192	$\alpha = 1.50,$ $\beta = -.91,$ $\omega = .21$	(.10, 2.71), (-2.15, 3.15), (.07, .61)
Minimum distance eaten to a cadaver (linear) $P_j = 1 - (1/1 + e^{-\alpha x_j^{\omega-\beta}})$	240.64	12.86	.001	$\alpha = .038,$ $\beta = .975$	(.002, .11), (.122, 1.38)
Null model (constant probability of infection)	247.88	20.10	3.48×10^{-5}	$P = .217$	(.17, .29)
Area eaten $P_j = 1 - \prod_{s=1}^{S_j} \eta$	249.65	21.88	1.43×10^{-5}	$\eta = .999957$	(.999953, .999961)

Note: The probability of infection given exposure is P_j . Note that in the models labeled “nonlinear,” the probability of infection is a nonlinear function of distance on a logit scale, whereas for the model labeled “linear,” the probability of infection is a linear function of distance on a logit scale.

model, additional bites at the same or greater distance had no effect on a larva’s overall risk of infection:

$$P_j = 1 - \frac{1}{1 + e^{-\alpha x_j^{\omega-\beta}}}. \tag{1}$$

Here x_j is the minimum distance between individual j ’s bites and a cadaver, and the variables α and β are fit parameters describing the effects of distance. Because the distribution of the virus around a cadaver may be quite complex, we also considered a model that includes the additional fit parameter ω to allow for more complex effects of distance:

$$P_j = 1 - \frac{1}{1 + e^{-\alpha x_j^{\omega-\beta}}}. \tag{2}$$

We also considered a model that neglects the effects of distance from a cadaver and instead allows only for the effects of area eaten. The probability of remaining uninfected after a single bite, η , is then the same for every cell, and so the probability of infection varies only with S_j , the number of bites eaten by individual j :

$$P_j = 1 - \prod_{s=1}^{S_j} \eta. \tag{3}$$

Finally, we allowed for both total area eaten and complex effects of distance at each bite:

$$P_j = 1 - \prod_{s=1}^{S_j} \frac{1}{1 + e^{-\alpha x_s^{\omega-\beta}}}. \tag{4}$$

Here S_j is again the total number of bites; x_s is the distance between bite s and a cadaver; and α , β , and ω are again fit parameters that describe the effects of distance. A cumulative model that omitted ω did not improve the fit of the model (results not shown).

Because larvae were effectively independent, we treated

them as independent Bernoulli trials (Ross 2005), with log likelihood calculated according to

$$L = \sum_{j=1}^{N_u} \ln(1 - P_j) + \sum_{j=1}^{N_i} \ln(P_j). \tag{5}$$

Here N_u and N_i are the number of uninfected and infected individuals at the end of the experiment (51 and 184, respectively), while P_j is determined by each successive model.

To maximize the likelihood, we used the multimln function of the GNU Scientific Library in the C programming language (Galassi et al. 2009). We then chose the best model using the AICc model selection criterion (Burnham and Anderson 2002), and we calculated confidence intervals by drawing 300 replicate sets of 235 leaf grids with replacement from the data and refitting the model to each replicate data set.

Results

In the best model, equation (4), the probability of infection depends on both the number of bites consumed at each distance and on complex effects of distance (table 1; all underlying data have been deposited in the Dryad Digital Repository: <http://doi.org/10.5061/dryad.q6h4n> [Eakin et al. 2014]). Because different selection criteria can sometimes give different results, in table A1 (tables A1–A4 available in the online appendix) we show that Bayesian information criterion (BIC) scores were virtually identical to the AICc scores. Infection risk is thus affected both by larval feeding history and the small-scale spatial distribution of the virus. Table 1 shows that there is also moderate support for the distance-only model, equation (2), further emphasizing the importance of distance from a cadaver on infection risk. Using the best-fit parameter estimates in the two best models then confirmed that the

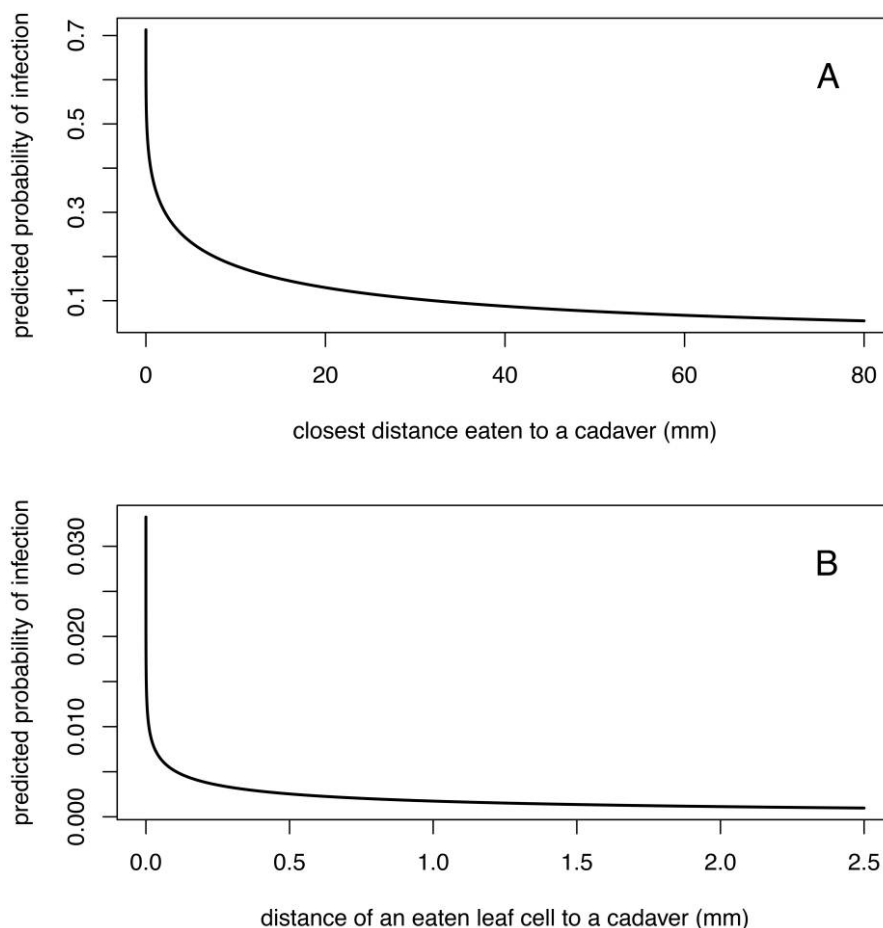


Figure 1: Probability of infection calculated using the two best models, equations (2) and (4). *A*, Probability per feeding bout. *B*, Probability per bite.

leaf area contaminated with virus is tightly localized around the cadaver (fig. 1).

Because the best model includes effects of both distance and number of bites, we can use it to understand the relative importance of each factor. When a caterpillar consumes a single bite of a cadaver, the distance to the cadaver is 0 mm, which in the best model gives a probability of infection of $1 - 1/(1 + \exp(-\beta))$. For our point estimate of β , the infection probability is 1.2%, and inserting the 95% confidence interval (CI) bounds on β into the model gives a range of 0.10%–4.7%. This estimate of infection probability given exposure may seem low, considering that cadavers consist almost entirely of infectious occlusion bodies. The average cadaver in our experiments, however, covered 78 grid cells, and so consumption of an entire cadaver would lead to an estimated probability of infection of 63%. Moreover, in our experiments, individual caterpillars on average consumed 5,250 bites, suggesting that

infection is typically due to the cumulative effects of consuming thousands of virus-contaminated leaf bits.

As a test of the best-fitting model, we calculated the infection probability for each larva by inserting the maximum likelihood estimates of the parameters into the best model. In figure 2, we plot these probabilities with shading to indicate which larvae actually became infected. As the figure shows, individuals with higher predicted probabilities of infection were indeed more likely to become infected. The model thus appears to assign a realistic probability of infection to each larva.

Modeling the Probability of Exposure

We next used our data to choose between competing models of feeding behavior. As in the probability of infection models, we focused on a small set of biologically plausible models that were based on many hours of observations.

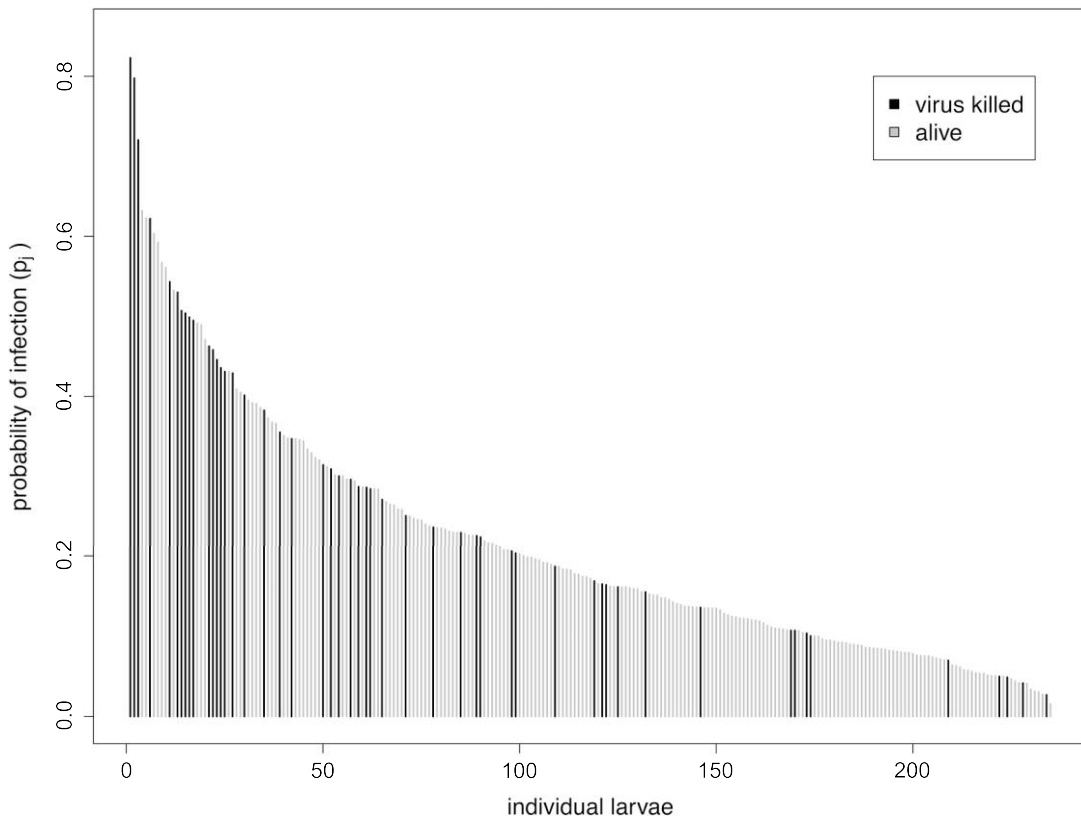


Figure 2: Predicted probability of infection for all 235 larvae in our data set, in rank order. Black bars = infected larvae; gray bars = surviving larvae.

Methods

Model Structure. During feeding, gypsy moth larvae use their prolegs to anchor themselves, leaving their forelegs free to bend or steady the part of the leaf that they are consuming. Larvae rarely chew through primary leaf veins, and after the first instar, they typically feed shallowly along the leaf edge (see fig. A2 for photographs of feeding damage). In accordance with this behavior, larvae in our models cannot consume larger leaf veins, they begin feeding on the leaf edge, and of course they cannot consume a leaf grid cell more than once. After the first bite, subsequent bites are chosen from the eight neighbors of the last cell consumed, which are together known as a Moore neighborhood (Deutsch and Dormann 2005).

To test for effects of cadaver avoidance, we used our data to choose between three different feeding algorithms. In the first model, which we include for purposes of comparison, larvae follow a random walk, while in the remaining two models, larvae show realistic behaviors, including limited movement while feeding and a preference for leaf edges. The third model then additionally includes cadaver avoidance. We therefore refer to the three models

as the random walk model, the no-avoidance model, and the cadaver-avoidance model.

To allow for different behaviors, the models assign different probabilities of consumption to the grid cells neighboring the last cell eaten. For example, in the random walk model, all cells neighboring the last cell eaten have an equal probability of being consumed. A simulated larva first chooses a random edge cell, after which the probability E_i of consuming neighboring cell i is

$$E_i = \frac{1}{Z}, \quad (6)$$

where Z is the number of uneaten neighbor cells.

In the two realistic algorithms, in contrast, each neighbor cell is weighted according to the cell's accessibility and the extent to which it is on the edge of the leaf. Accessibility is determined by the area that a larva can reach without shifting its position on the leaf, which in the model is a circle of radius r mm around current center point C . Within this circle, the probability of consuming a given cell i declines with increasing distance D_i from C . Therefore, we calculate the first weight $w_{1,i}$ as

$$w_{1,i} = 1 - \frac{1}{1 + e^{-\rho_1 D_i}}, \quad (7)$$

The radius r and the parameter ρ_1 were then both fit to the data. If there are no available cells within a distance r of point C , the simulated larva shifts its position by choosing, as a new center point, the nonempty cell that is closest to the current center point C .

The second weight then allows for the extent to which each neighbor cell is preferred based on its proximity to the edge of a leaf, according to its number of empty neighbors h_i . To allow for the possibility of complex effects of h_i on feeding, we assume that this weight is a power function of h_i , normalized by the values assigned to all nonempty neighbors:

$$w_{2,i} = \frac{h_i^{\rho_2}}{\sum_{j=1}^Z h_j^{\rho_2}}. \quad (8)$$

Here Z is the total number of nonempty cells neighboring the last cell eaten, and ρ_2 is fit to the data.

The algorithms then combine the two weights $w_{1,i}$ and $w_{2,i}$ into an overall probability E_i of eating neighbor cell i :

$$E_i = \frac{w_{1,i} w_{2,i}}{\sum_{j=1}^Z w_{1,j} w_{2,j}}. \quad (9)$$

If a simulated larva eats a cell that has no consumable neighbors, the algorithm searches for the nearest available nonneighbor. The larva then eats that cell, and the simulation continues.

In the cadaver-avoidance model, we also calculate the probability of cadaver avoidance A_i :

$$A_i = 1 - \frac{1}{1 + e^{-\gamma x_i - \kappa}}. \quad (10)$$

Here x_i is the Euclidean distance between cell i and the closest cadaver cell, so that the probability of detection declines with distance from a cadaver, as observed in choice tests (Parker et al. 2010). If A_i is larger than a random variate drawn from a uniform distribution between 0 and 1, then the simulated larva detects the cadaver and instead chooses a bite that is farther from the cadaver. If there are multiple neighbor cells that are equally far from the cadaver, then the algorithm chooses among them with equal probability. The parameters γ and κ are then fit to the data.

For each leaf in our data set, each simulated larva eats the same amount as the observed larva, starting at the centermost edge cell of the observed bout. To ensure that leaves with more bouts did not have a disproportionate influence, we used only one bout per leaf. In each case, we selected the bout closest to a cadaver because otherwise

there would have been little chance of detecting cadaver avoidance. Not every larva in our experiments fed close to a cadaver, however, and so the bouts that we used were located at a range of distances from cadavers (fig. A5).

Choosing the Best Feeding Model. To choose between feeding models, we again used maximum likelihood and AIC analysis. Our ability to make inferences about the feeding models, however, was constrained by computing speed, as is often the case with stochastic simulations in ecology (Hartig et al. 2011). The underlying problem is that, for the feeding models, there is no closed-form expression describing the probability of different model outcomes in terms of the model parameters, as there was for the probability of infection models. Therefore, we were forced to estimate the probability of different model outcomes by simulating the models many times for each set of possible parameter values.

We first attempted to carry out a pixel-by-pixel comparison of model leaves to data leaves using an integrated likelihood (Berger et al. 1999). In practice, this meant averaging likelihoods across model realizations (Ross 2002), but accurate estimation of the average turned out to require a prohibitive number of realizations. Therefore, we instead compared summary statistics from the model to summary statistics from the data, and we used kernel density estimation to interpolate a continuous probability distribution of model outcomes from a modest number of realizations (Hartig et al. 2011).

The two summary statistics that we used were the perimeter and the predicted probability of infection for each feeding bout. We used the perimeter because our simulated bouts have the same number of bites as the corresponding real bout, and so each combination of model bout and real bout has the same area. If two bouts also have the same perimeter, then by elementary geometry they will have similar shapes. We therefore expected that the perimeters of model feeding bouts would be informative about the fit of the models to the data.

A bout's perimeter, however, contains little information about its location on a leaf, and so using the perimeter alone resulted in model feeding bouts that were of similar shape to the real bout but not in the same location, thus providing a poor match to real feeding bouts. We therefore included a second summary statistic, the predicted probability of infection for each bout, as calculated using the best probability of infection model, equation (4). The predicted probability of infection usefully complements the perimeter because two feeding bouts of similar shape and location will have similar probabilities of infection, whereas if the two bouts have similar shape but different locations, they will likely have quite different probabilities of infection.

In using kernel density estimation to calculate the prob-

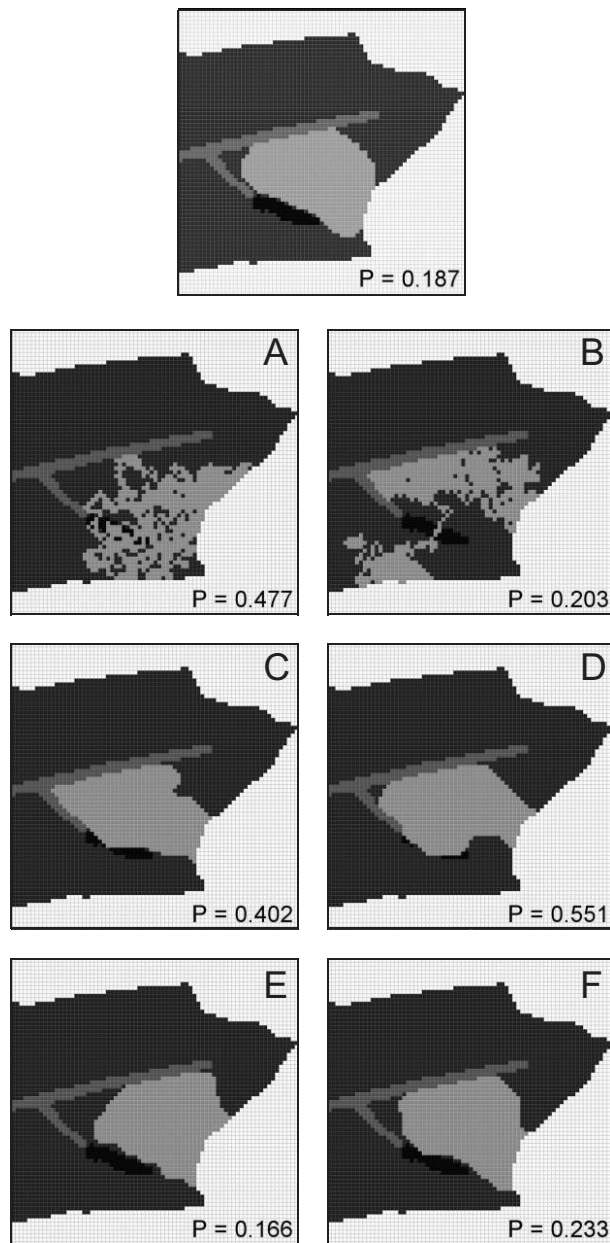


Figure 3: Feeding bouts created using the three larval feeding algorithms. P is the predicted probability of infection, calculated using equation (4). *Top grid*, real feeding bout, followed by pairs of realizations for the random walk model (A, B), the no-avoidance model (C, D), and the avoidance model (E, F). For each grid, the feeding bout is light gray, the cadaver is black, and the leaf vein and uneaten leaf area are gray and dark gray, respectively.

ability of each statistic, an important consideration was that the two statistics are scaled differently, in that the probability of infection is constrained to fall between 0 and 1, whereas the perimeter is not. If we had used a two-dimensional kernel, this difference in scaling would likely

have required the use of a complex prewhitening routine to avoid biased estimation (Silverman 1986). Moreover, the number of computations needed to estimate a single multidimensional kernel is often much higher than the number needed to estimate one kernel for each dimension (Silverman 1986). Therefore, we followed a standard recommendation in using a so-called product kernel, which in our case meant using a two-dimensional kernel that is expressed as the product of two one-dimensional kernels (Scott 1992; Scott and Sain 2005)

In practice, this meant that for a given set of parameter values and a given feeding bout from our data set, we first generated 1,000 realized feeding bouts, recording the perimeter and the probability of infection for each bout. We then used two one-dimensional kernel density estimation routines to turn the 1,000 realized values of each statistic into a pair of smooth probability distribution functions, and we summed the log probability of the two statistics to calculate an overall likelihood:

$$L_{jk} = \log(P_{pm,jk}) + \log(P_{pi,jk}). \quad (11)$$

Here $P_{pm,jk}$ is the probability of the observed perimeter pm for real feeding bout j , as calculated from model perimeters generated with parameter set k . Similarly, $P_{pi,jk}$ is the probability of the infection pi for real feeding bout j , again as calculated from the distribution of infection probabilities generated with parameter set k . We then maximized the log likelihoods using a Nelder-Mead downhill simplex algorithm (Press et al. 1992), and we again used AICc analysis to choose the best model.

Using a product kernel is equivalent to assuming that perimeters and probabilities of infection are independent, an assumption that is unlikely to be exactly correct. Preliminary analyses nevertheless showed that the correlation between the two statistics is rather weak (correlation coefficient $\rho = 0.315$, 95% CI = [0.195, 0.426]), as we would expect if the two statistics are both informative about the fit of the model to the data. It thus seemed likely that assuming that the summary statistics are independent would not strongly affect our conclusions.

To test this assumption in particular and our fitting routine in general, we repeatedly fit the best model to an artificial data set generated by inserting the best-fit parameters into the model, following standard practice (Bolker 2008). To do this, we first generated 235 artificial feeding bouts, the same number as in the original data set, using the maximum likelihood estimates of the parameters. We then fit the model to this artificial data set 300 times. The mean for each parameter was quite close to the value used to generate the artificial data set (table A4). Therefore, we are reasonably confident that our fitting routines are not biased and that the weak correlation be-

Table 2: Corrected Akaike information criterion (AICc) scores, maximum likelihood estimates, and bootstrapped 95% confidence intervals (CIs) for our feeding algorithms

Model	AICc	Δ AICc	AICc weight	Parameters	95% CI
Cadaver avoidance (eqq. [7]–[10])	2,865.70	.0	1.0	$\rho_1 = 1.16 \text{ mm}^{-1}$, $r = .21 \text{ cm}$, $\rho_2 = 15.27$, $\gamma = 20.03 \text{ mm}^{-1}$, $\kappa = 16.22$	(.76, 1.74), (.13, .31), (11.84, 18.18), (12.05, 32.72), (6.62, 33.20)
No avoidance (eqq. [7]–[9])	3,115.74	Median: 88.9, range: 15.8–250	.0	$\rho_1 = 1.01 \text{ mm}^{-1}$, $r = .23 \text{ cm}$, $\rho_2 = 12.53$	(.56, 2.22), (.11, .40), (9.45, 19.85)

Note: The parameters ρ_1 and r describe the localized feeding of larvae, ρ_2 determines the extent to which larvae prefer grid cells that are on the edge of a leaf, and γ and κ are cadaver-avoidance parameters. Note that the AICc weights for the model without avoidance are very close to zero for the entire range of AICc scores.

tween perimeters and probabilities of infection had little effect on our conclusions.

A final point is that our likelihood calculations were dependent on our estimates of the parameters α , β , and ω of the probability of infection model, equation (4), and these estimates, of course, have associated uncertainties. To take these uncertainties into account, we used the 300 bootstrapped parameter values that we had earlier used to create confidence intervals for each parameter of the feeding models by repeating our maximum likelihood calculation for each of the 300 bootstrapped sets of α , β , and ω . We therefore report both the median and the range of the AICc across these 300 parameter sets, as well as the range of AICc differences. The resulting model selection procedure is somewhat informal, but the cadaver-avoidance model fit the data so much better than the no-avoidance model that we believe that our conclusions are robust. Nevertheless, the 95% confidence intervals on the parameter estimates of the feeding models were calculated across the 300 sets of values of α , β , and ω , a procedure that is sufficiently informal that the confidence intervals may not reflect the true uncertainty in the parameters.

Results

Because our feeding models are stochastic, we do not expect them to exactly reproduce the original feeding bouts. Nevertheless, each of the two realistic models produces bouts that are similar to the original bouts (fig. 3; all 235 bouts are shown in figs. A6–A8). Because the random walk algorithm provides a very poor fit to the data, we do not consider it in model selection.

Moreover, as figure 3 emphasizes, the model with cadaver avoidance provides a much better fit to the data than does the model without avoidance, such that the median AICc difference is 88.9 and the range of AICc differences is 15.8–250.0 (table 2; also, table A2 shows that the BIC scores were again virtually identical). Given that

AICc differences larger than 7 indicate that there is overwhelming evidence for the best model (Burnham and Anderson 2002), the model with cadaver avoidance clearly provides a better explanation of the data for all 300 sets of the probability of infection parameters α , β , and ω . We also note that the maximum likelihood estimates for the three parameters shared by the two realistic algorithms, r , ρ_1 , and ρ_2 , are not significantly different between the two models, which supports our argument that the better fit of the cadaver-avoidance model is not simply due to that model having more parameters. Our experimental data thus allow us to clearly distinguish between the two models. We therefore conclude that our data provide very strong evidence that cadaver avoidance alters the feeding behavior of gypsy moth larvae.

Figure 4 then shows that the cadaver-avoidance model predicts a sharp decline in detection probability beginning at about 0.7 mm from a cadaver. The probability that a larva detects a cadaver is thus low until the larva is close to the cadaver. As we will show, however, this short detection distance is sufficient to substantially lower infection risk.

Testing the Model Predictions

Methods

The final step in our research was to combine our feeding models with our probability of infection models and to use the combined models to make predictions of infection risk, thereby testing whether cadaver avoidance does in fact reduce a larva's infection risk. Ultimately, we hope to also understand the effects of cadaver avoidance on epizootics and gypsy moth outbreaks, but as a first step we consider only a single round of transmission. Moreover, allowing for only a single round of transmission allowed us to compare model predictions to data from field experiments that similarly allowed for only a single round of transmission (Elder et al. 2008). In the field experi-

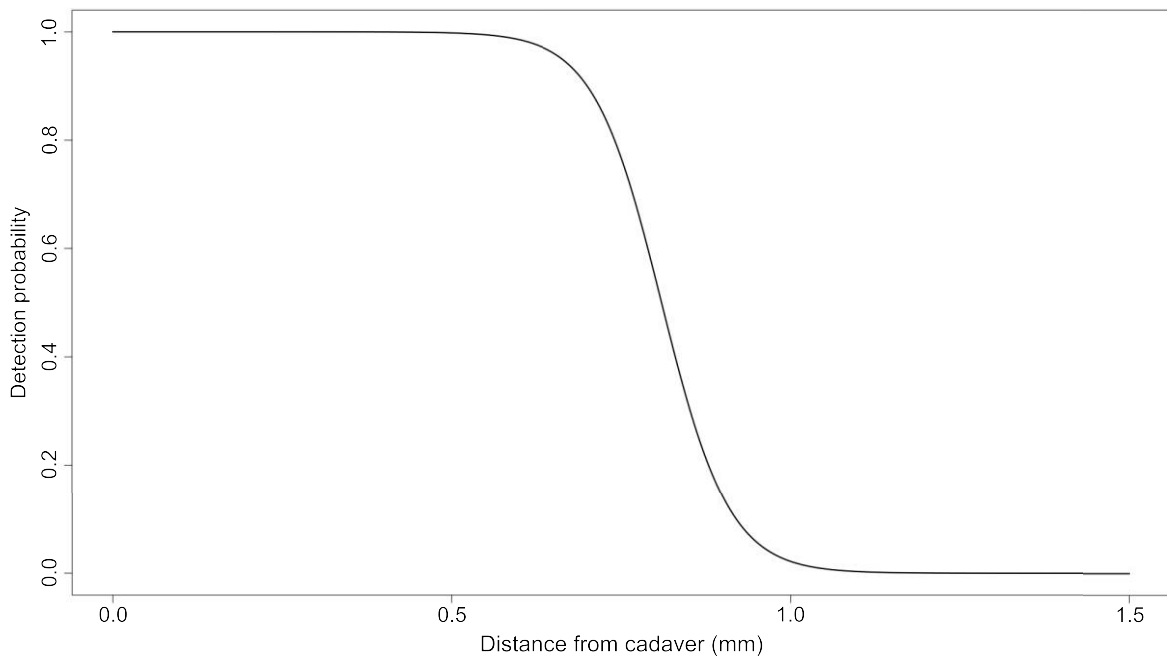


Figure 4: Detection probability versus distance from a cadaver, as calculated by the detection model, equation (10), using the maximum likelihood estimates for the parameters γ and κ .

ments, 25 uninfected fourth instars were allowed to feed for a week on 40-leaf branches, which were contaminated with a known density of infected first-instar larvae. The infection rate was measured as the fraction of larvae that became infected on each branch. Comparing the model predictions to the data then required that we scale up our feeding models to allow for multiple leaves and multiple larvae (appendix).

Results

Comparing the models to the field data shows that the cadaver-avoidance model has $r^2 = 0.51$, while the no-avoidance model has $r^2 = 0.48$, and the random walk model has $r^2 = 0.39$ (fig. 5). The models thus explain a reasonably high fraction of the variance in the field data, especially given that they are making a priori predictions. We therefore conclude that our models and experiments together provide a realistic description of the effects of gypsy moth larval feeding behavior on virus infection risk.

Part of the reason why the models do not fit the field data better is that the curvature of the function relating infection risk to virus density is strongly affected by innate variation in infection risk between individuals (Dwyer et al. 1997). We did not include such variation in our models first because estimating its effects would have made our fitting routines prohibitively slow. Moreover, it is more

biologically illuminating to compare models that differed only in feeding behavior rather than in variability across individuals. This is because changes in the curvature of the infection risk function have previously been attributed to variability between individuals that is due either to genetic differences between larvae (Elder et al. 2008) or induced changes in hydrolyzable tannins (Elder et al. 2013). Figure 5 in contrast shows that changes in feeding behavior alone can also affect the curvature of the function, and comparisons between feeding models shows that this curvature is affected by multiple aspects of feeding. First, the no-avoidance model reduces the rate at which the infection rate increases with increasing virus density relative to the random walk model, showing that a preference for edges and nearby leaf tissue can alter the curvature of the infection rate function. Second, the cadaver-avoidance model similarly reduces the rate at which the infection rate increases with increasing virus density, showing that cadaver avoidance likewise alters the curvature of the infection rate function. These effects most likely occur because larvae vary in their proximity to a cadaver, just as they may vary due to differing genetic backgrounds or to changes in hydrolyzable tannin levels.

Given that our overall goal was to test whether cadaver avoidance affects infection risk, the most important feature of figure 5 is that the cadaver-avoidance model predicts lower infection rates than either the random walk model

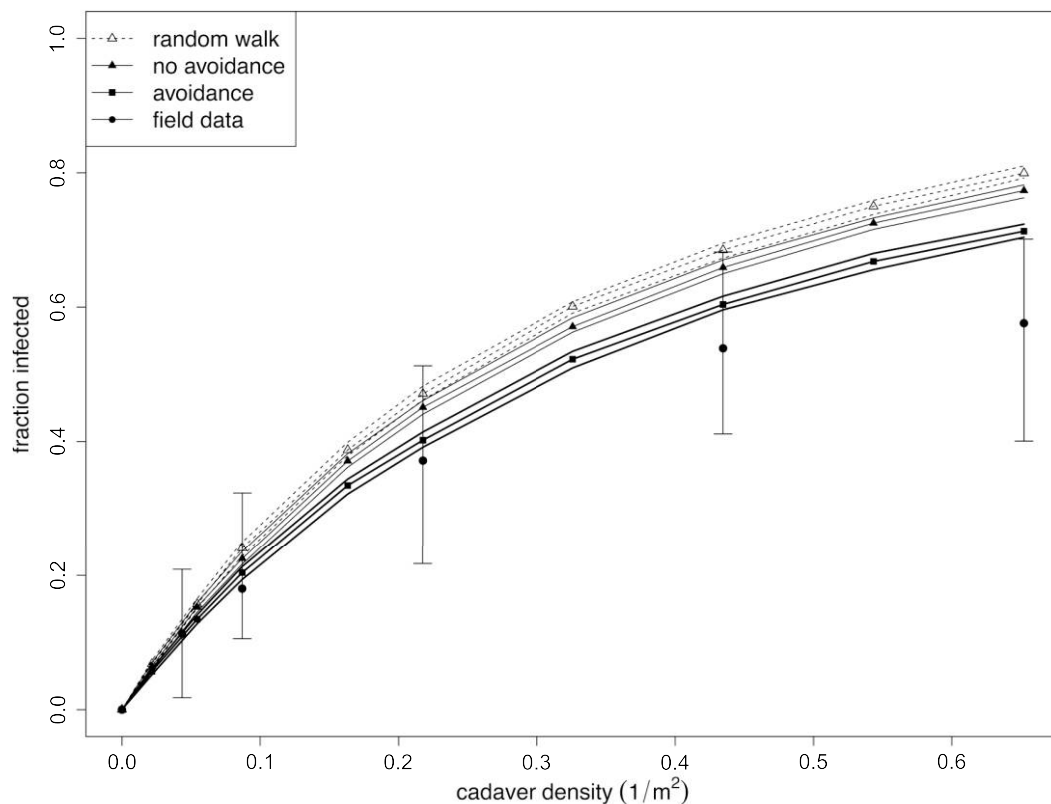


Figure 5: Predicted fraction infected for each feeding model (lines with points indicate the median and the 95th percentile range) versus the data (points with bars indicate 50th percentile ranges).

or the no-avoidance model, implying that cadaver avoidance does indeed reduce infection risk. Relative to the no-avoidance model, the cadaver-avoidance model reduces infection rates by about 4% across virus densities and by roughly 7% at the highest virus density. Although these differences may seem modest, they were calculated over only a single round of transmission, whereas naturally occurring epizootics typically have multiple rounds of transmission (Woods and Elkinton 1987). Scaling the realistic models up to allow for entire epizootics confirmed that avoidance behavior also has strong effects on epizootics (Eakin 2012), as we will detail in a future publication. We therefore conclude that cadaver avoidance substantially reduces the risk that a gypsy moth larva will become infected with the gypsy moth baculovirus.

Discussion

To our knowledge, our work provides the first demonstration that cadaver avoidance alters an insect's risk of infection with a baculovirus (but see Vasconcelos et al. 1996) for differences in movement rates between healthy

and infected larvae of the cabbage moth *Mamestra brassicae*). Our work also shows that spatial structure at the scale of millimeters affects the transmission of this virus, which is a smaller scale than has previously been reported for baculoviruses of this or other insects (Dwyer 1991; Vasconcelos et al. 1996; D'Amico et al. 2005). More broadly, our work provides one of the most direct quantifications to date of the effect of a host's behavior on its risk of pathogen infection. Our estimate is nevertheless somewhat indirect because it is based on a difference in model predictions, but in contrast to previous studies, our use of model predictions meant that we did not have to eliminate avoidance behavior to demonstrate that avoidance behavior affects risk (Kendall et al. 1999; Behringer et al. 2006). Moreover, combining models and experiments allowed us to understand how individual behaviors are translated into infection risk.

For insect-baculovirus interactions, efforts to understand transmission typically use dose-response experiments, in which larvae that do not consume the entire dose are discarded, so that there is again no effect of feeding behavior (Cory and Myers 2003). Partly as a result,

dose-response experiments cannot always be used to predict infection rates in the field (Dwyer et al. 2005). Field experiments, in contrast, can be used to predict infection rates in nature (Dwyer et al. 1997) but do not allow for a mechanistic understanding of transmission. Our experiments thus provide a deeper mechanistic understanding of baculovirus transmission than either dose-response or field experiments, and we therefore argue that future research on baculovirus transmission should similarly consider the probability of exposure. Moreover, given that baculovirus biology is quite similar across insect hosts, models similar to ours may be useful for understanding transmission in other insect-baculovirus interactions.

Because cadaver avoidance is heritable in choice tests (Parker et al. 2010), it seems likely that it is also heritable when larvae are allowed to feed more naturally, as in our experiments. Moreover, because previous work has shown that natural selection on overall infection risk helps drive gypsy moth outbreaks (Elder et al. 2008), we suspect that selection on cadaver avoidance affects outbreaks. The levels of cadaver avoidance shown by gypsy moth larvae, however, likely reflect a trade-off between avoidance and feeding rates, because lower avoidance rates may permit more continuous feeding and, thus, higher fecundity (Hough and Pimentel 1978). As evidence in support of this argument, we note that we observed no difference in feeding rates on contaminated and uncontaminated leaves and that our best model predicts that a larva will only avoid a cadaver if the cadaver is only a few millimeters away. These results together suggest that there is strong selection for larvae to not interrupt their feeding until they are very close to cadavers. Our models further suggest that infection does not occur unless a larva consumes many contaminated bits of leaf, and so physiological resistance may allow larvae to feed very close to cadavers without becoming infected.

Thus, one of the implications of our work is that infection is affected by spatial variability both in exposure risk and in infection risk given exposure. This is important, partly because it seems likely that cadaver avoidance and physiological resistance are determined by different genes and therefore may evolve independently. Additionally, when baculoviruses are sprayed as insecticides (Moreau and Lucarotti 2007), the virus is distributed more or less uniformly over the foliage (Webb et al. 1990), whereas in natural epizootics, cadavers occur as dense clumps of occlusion bodies. Shortly after a spray application, it may therefore be very difficult for larvae to avoid the virus, and so spray applications may impose a different selection pressure than natural epizootics.

Our work suggests that stochastic simulation models can usefully complement ordinary differential equation models in disease ecology. While partial differential equa-

tion models can similarly be useful for studying the ecological consequences of behavior (Kareiva and Odell 1987), in our case it would have been very difficult to write down a realistic partial differential equation model. In partial differential equation models of behavior, animal density changes either because of births and deaths or because of dispersal between locations (Murray 1989). In baculovirus transmission, in contrast, larvae consume the leaves on which they are moving, and so the density of larvae and cadavers changes because the landscape is effectively shrinking. Allowing for such a process would be very difficult in a partial differential equation, but it is straightforward in a computer algorithm. Our work, therefore, adds to the growing consensus that stochastic simulation models have a useful role to play in disease ecology (Longini et al. 2005).

Acknowledgments

L.E. thanks J. Crnich, S. and P. Eakin, B. Elder, E. Fuller, A. Hunter, D. Kennedy, and B. Parker for help with data collection and analysis. Our work was supported by National Institutes of Health grant R01GM096655 to G.D., V. Dukic, and B. Rehill. G.D. thanks V. Dukic for useful discussions of model-selection procedures. We also thank the staff of the Kellogg Biological Station. Associate Editor K. Gross, reviewer L. Johnson, and an anonymous reviewer made many helpful comments on the manuscript.

Literature Cited

- Anderson, R. M., and R. M. May. 1992. *Infectious diseases of humans: dynamics and control*. Oxford University Press, New York.
- Antolin, M. F. 2008. Unpacking beta: within-host dynamics and the evolutionary ecology of pathogen transmission. *Annual Review of Ecology, Evolution, and Systematics* 39:415–437.
- Behringer, D. C., M. J. Butler, and J. D. Shields. 2006. Avoidance of disease by social lobsters. *Nature* 441:421.
- Berger, J. O., B. Liseo, and R. L. Wolpert. 1999. Integrated likelihood methods for eliminating nuisance parameters. *Statistical Science* 14:1–22.
- Bolker, B. M. 2008. *Ecological models and data* in R. Princeton University Press, Princeton, NJ.
- Bolker, B. M., M. E. Brooks, C. J. Clark, S. W. Genage, J. R. Poulsen, H. H. Stevens, and J. S. White. 2009. Generalized linear mixed models: a practical guide for ecology and evolution. *Trends in Ecology and Evolution* 24:127–135.
- Bouwman, K. M., and D. M. Hawley. 2010. Sickness behaviour acting as an evolutionary trap? male house finches preferentially feed near diseased conspecifics. *Biology Letters* 6:462–465.
- Burnham, K. P., and D. R. Anderson. 2002. *Model selection and multimodel inference: a practical information-theoretic approach*. Springer, Berlin.
- Capinera, J. L., S. P. Kirouac, and P. Barbosa. 1976. Phagodeterrence

- of cadaver components to gypsy moth larvae, *Lymantria dispar*. *Journal of Invertebrate Pathology* 28:277–279.
- Civitello, D. J., S. Pearsall, M. A. Duffy, and S. R. Hall. 2013. Parasite consumption and host interference can inhibit disease spread in dense populations. *Ecology Letters* 16:626–634.
- Cory, J. S., and J. H. Myers. 2003. The ecology and evolution of insect baculoviruses. *Annual Reviews of Ecology and Systematics* 34:239–272.
- D'Amico, V., J. Elkinton, J. D. Podgwaite, J. P. Buonaccorsi, and G. Dwyer. 2005. Pathogen clumping: an explanation for non-linear transmission of an insect. *Ecological Entomology* 30:383–390.
- Deutsch, A., and S. Dormann. 2005. Cellular automaton modeling of biological pattern formation. Birkhäuser, Boston.
- Dwyer, G. 1991. The roles of density, stage and patchiness in the transmission of an insect virus. *Ecology* 72:559–574.
- Dwyer, G., J. Dushoff, and S. H. Yee. 2004. The combined effects of pathogens and predators on insect outbreaks. *Nature* 430:341–345.
- Dwyer, G., J. Elkinton, and J. P. Buonaccorsi. 1997. Host heterogeneity in susceptibility and disease dynamics: tests of a mathematical model. *American Naturalist* 150:685–707.
- Dwyer, G., J. Firestone, and T. E. Stevens. 2005. Should models of disease dynamics in herbivorous insects include the effects of variability in host-plant foliage quality? *American Naturalist* 165:16–31.
- Eakin, L., M. Wang, and G. Dwyer. 2014. Data from: The effects of the avoidance of infectious hosts on infection risk in an insect-pathogen interaction. *American Naturalist*, Dryad Digital Repository, <http://doi.org/10.5061/dryad.q6h4n>.
- Eakin, L. E. 2012. Defining the scale of cadaver avoidance in gypsy moths, *Lymantria dispar*. PhD diss. University of Chicago, Chicago.
- Elder, B. D., J. Dushoff, and G. Dwyer. 2008. Host-pathogen interactions, insect outbreaks, and natural selection for disease resistance. *American Naturalist* 172:829–842.
- Elder, B. D., B. J. Rehill, K. J. Haynes, and G. Dwyer. 2013. Induced plant defenses, host-pathogen interactions, and forest insect outbreaks. *Proceedings of the National Academy of Sciences of the USA* 110:14978–14983.
- Elkinton, J. S., and A. M. Liebhold. 1990. Population dynamics of gypsy moth in North America. *Annual Review of Entomology* 35:571–596.
- Galassi, M., J. Davies, J. Theiler, B. Gough, G. Jungman, P. Alken, M. Booth, and F. Rossi. 2009. GNU scientific library reference manual. 3rd ed. Network Theory, Bristol, UK.
- Hartig, E., J. M. Calabrese, B. Reineking, T. Wiegand, and A. Huth. 2011. Statistical inference for stochastic simulation models—theory and application. *Ecology Letters* 14:816–827.
- Hawley, D. M., R. S. Etienne, V. O. Ezenwa, and A. E. Jolles. 2011. Does animal behavior underlie covariation between hosts' exposure to infectious agents and susceptibility to infection? implications for disease dynamics. *Integrative and Comparative Biology* 51:528–539.
- Hosseini, P., A. Dhondt, and A. Dobson. 2004. Seasonality and wild-life disease: how seasonal birth, aggregation and variation in immunity affect the dynamics of *Mycoplasma gallisepticum* in house finches. *Proceedings of the Royal Society B: Biological Sciences* 271:2569–2577.
- Hough, J., and D. Pimentel. 1978. Influence of host foliage on development, survival, and fecundity of the gypsy moth. *Environmental Entomology* 7:97–102.
- Kareiva, P., and G. Odell. 1987. Swarms of predators exhibit “prey-taxis” if individual predators use area-restricted search. *American Naturalist* 130:233–270.
- Keeling, M. J., and P. Rohani. 2007. Modeling infectious diseases in humans and animals. Princeton University Press, Princeton, NJ.
- Kendall, B. E., C. J. Briggs, W. W. Murdoch, P. Turchin, S. P. Ellner, E. McCauley, R. M. Nisbet, and S. N. Wood. 1999. Why do populations cycle? a synthesis of statistical and mechanistic modeling approaches. *Ecology* 80:1789–1805.
- Kiesecker, J. M., D. K. Skelly, K. H. Beard, and E. Preisser. 1999. Behavioral reduction of infection risk. *Proceedings of the National Academy of Sciences of the USA* 96:9165–9168.
- Longini, I. M., A. Nizam, S. Xu, K. Ungchusak, W. Hanshaworakul, D. A. T. Cummings, and M. E. Halloran. 2005. Containing pandemic influenza at the source. *Science* 309:1083–1087.
- McManus, M. L., and T. McIntyre. 1981. Introduction. Pages 1–7 in C. Doane and M. McManus, eds. *The gypsy moth: research toward integrated pest management*. USDA, Washington, DC.
- Moreau, G., and C. J. Lucarotti. 2007. A brief review of the past use of baculoviruses for the management of eruptive forest defoliators and recent developments on a sawfly virus in Canada. *Forestry Chronicle* 83:105–112.
- Murray, J. D. 1989. *Mathematical biology*. Springer, Berlin.
- Parker, B. J., S. M. Barribeau, A. M. Laughton, J. C. de Roode, and N. M. Gerardo. 2011. Non-immunological defense in an evolutionary framework. *Trends in Ecology and Evolution* 26:242–248.
- Parker, B. J., B. D. Elder, and G. Dwyer. 2010. Host behaviour and exposure risk in an insect-pathogen interaction. *Journal of Animal Ecology* 79:863–870.
- Press, W. H., S. A. Teukolsky, W. T. Vetterling, and B. P. Flannery. 1992. *Numerical recipes in C: the art of scientific computing*. Cambridge University Press, Cambridge.
- Ross, S. 2002. *Simulation*. 3rd ed. Academic Press, Waltham, MA.
- Ross, S. M. 2005. *A first course in probability*. 7th ed. Prentice Hall, Chestnut Hill, MA.
- Scott, D. W. 1992. *Multivariate density estimation: theory, practice and visualization*. Wiley, New York.
- Scott, D. W., and S. Sain. 2005. *Handbook of statistics*. Vol. 24. Data mining and computational statistics, chapter multi-dimensional density estimation. Elsevier, Amsterdam.
- Silverman, B. W. 1986. *Density estimation for statistics and data analysis*. Chapman & Hall, London.
- Vasconcelos, S. D., J. S. Cory, K. R. Wilson, S. M. Sait, and R. S. Hails. 1996. Modified behavior in baculovirus-infected lepidopteran larvae and its impact on the spatial distribution of inoculum. *Biological Control* 7:299–306.
- Webb, R. E., J. D. Podgwaite, M. Shapiro, K. M. Tatman, and L. W. Douglass. 1990. Hydraulic spray application of Gypcheck as a homeowner control tactic against gypsy moth (Lepidoptera: Lymantriidae). *Journal of Entomological Science* 25:383–393.
- Webb, R. E., G. B. White, J. D. Podgwaite, V. D'Amico, J. Slavicek, J. Swearingen, B. Onken, and K. W. Thorpe. 2005. Comparison of aerially-applied Gypcheck strains against gypsy moth (Lepidoptera: Lymantriidae) in the presence of an *Entomophaga maimaiga* epizootic. *Journal of Entomological Science* 40:446–460.
- Woods, S. A., and J. S. Elkinton. 1987. Bimodal patterns of mortality from nuclear polyhedrosis virus in gypsy moth (*Lymantria dispar*) populations. *Journal of Invertebrate Pathology* 50:151–157.

Associate Editor: Kevin Gross
 Editor: Susan Kalisz